1-D particle-in-cell simulations of electron acoustic solitary structures in an electron beam-plasma

Cite as: AIP Advances **9**, 025029 (2019); https://doi.org/10.1063/1.5080757
Submitted: 12 November 2018 . Accepted: 18 February 2019 . Published Online: 26 February 2019

A. A. Abid, Quanming Lu, M. N. S. Qureshi, X. L. Gao, Huayue Chen, K. H. Shah, and Shui Wang

1-D particle-in-cell simulations of electron acoustic solitary structures in an electron beam-plasma

Cite as: AIP Advances 9, 025029 (2019); doi: 10.1063/1.5080757
Submitted: 12 November 2018 • Accepted: 18 February 2019 •
Published Online: 26 February 2019

A. A. Abid,[1,a] Quanming Lu,[1,a] M. N. S. Qureshi,[2] X. L. Gao,[1] Huayue Chen,[1] K. H. Shah,[3] and Shui Wang[1]

AFFILIATIONS

[1]CAS Key Laboratory of Geospace Environment, Department of Geophysics and Planetary Science, University of Science and Technology of China, Hefei 23006, China
[2]Department of Physics, GC University, Lahore 54000, Pakistan
[3]Department of Physics, Forman Christian College (A Charted University), Lahore 54600, Pakistan

[a]Email: abidaliabid1@hotmail.com; qmlu@ustc.edu.cn

ABSTRACT

Electrostatic solitary (ES) structures have been frequently observed in the solar wind, Earth's and other planetary magnetosphere and are the most widely theoretically studied waves in literature. However, there are very few studies in which simulations and theoretical studies have been performed simultaneously. In this paper, we perform 1-D electrostatic Particle-in-Cell (PIC) simulations of electrostatic solitary (ES) waves in a plasma which consists of **immobile ions**, and cold, beam and hot electrons. It is found that for a small value of electron beam velocity, ES structures are formed due to the steepening of initially quasi monochromatic electron acoustic (EA) waves. We interpret these ES structures as electron acoustic solitary (EAS) structures, which **agree** with the rarefactive (negative electrostatic potential) electron acoustic solitary structures obtained **theoretically** as a solution of the Korteweg de-Vries (KdV) equation. **We found that polarity of solitary structures depends on the drift velocity of electron beam and formation of electric field spikes are consistent with the ES waves observations from Earth's magnetosphere**.

I. INTRODUCTION

Electrostatic solitary (ES) waves have been **frequently** observed in the Earth's magnetosphere, such as in the magnetosheath,[1] the plasma sheet boundary layer,[2,3] the bow shock,[4] strong currents in the auroral acceleration region[5,6] and in the solar wind.[7] Generally two types of ES structures have been found in the space plasmas, compressive solitary structure and **rarefactive** solitary structure.[8] The compressive solitary structures basically correspond to positive electrostatic potentials.[9] In the plasma sheet boundary layer, propagating velocities of such compressive solitary structures parallel to the background magnetic field are found to be of few thousand km/s.[10–12] It has been found that these compressive solitary structures may arise due to the two stream instability, bump on tail instability[10] or **electron acoustic (EA) waves** generated in electron beam plasma.[7,13–15] On the other hand, the rarefactive solitary structures exhibit negative electrostatic potential.[8,16,17] The scales of these negative potential structures are nearly similar to the dispersive scale of electron-acoustic (EA) waves.[14,18,19] Later, it has been found that the rarefactive solitary structures are manifestation of steepened EA waves.[19]

The EA waves generally exist in the presence of hot and cold electron where the ratio of hot and cold electron temperatures is more than 10^{13}. It has been found by many authors[12–14] that the linear behavior of EA waves is similar to linear behavior of ion acoustic (IA) waves. The cold electrons in EA waves play a similar role as ions do in IA waves.[12] There have been several theoretical attempts to clarify the broadband-electrostatic-noise (BEN) observed in different parts of the Earth's magnetosphere which are associated with the EA waves. Verheest et al.[8] found compressive

electron acoustic solitary (EAS) structures, in the absence of electron beam component. Berthomier et al.[16] investigated the EAS waves in the presence of the electron beam by employing Sagdeev potential technique. The propagating velocities of these EA solitons in their study were strongly associated with the beam velocity. In an unmagnetized plasma system, nonlinear behavior of EA waves were studied by KdV equation[10,17,18] and analytical results showed that EA waves evolve into EAS structure when their amplitude is large. El-labany and co-worker[19] studied the EAS structure in the presence of beam electrons and found that not only rarefactive structures but compressive solitary structures can also be obtained for EAS waves. The change in polarity of the solitary structure depends on the drift velocity of electron-beam. More recently Shah et al.[18] revised the nonlinear effects of EA waves by employing non-Maxwellian distribution function and found that both rarefactive and compressive solitary structures can be obtained for EA when electrons follow the generalized (r, q) distribution function.

In this manuscript, we first studied the electron acoustic solitary (EAS) wave theoretically and then with 1D particle-in-cell (PIC) simulations. We have investigated the steepening of EA waves in a plasma system, whose constituents are hot, cold and beam electrons. The formation of rarefactive EAS structure due to steepening of EA waves by PIC simulations supported up by theoretical formulism have not been discussed before according to the best of our knowledge. The paper is systematized as follows: In Sec. II, we present a theoretical model for an unmagnetized three component plasma and derived Kortewag de-Varies (KdV) equation for the EAS structures. In Sec. III, we present simulation setup for three component plasma and results for the formation of EAS structures. Finally, the main conclusion of this manuscript has been recapitulated in Sec. IV.

II. THEORETICAL MODEL

We consider an unmagnetized plasma consisting of **static ions**, three Maxwellian electron populations: non-drifting cold and hot populations and third one is the electron beam with an equilibrium velocity v_{b0}. The fundamental set of normalized fluid equations describing the propagation of electron acoustic waves, in 1D, are

$$\frac{\partial n_c}{\partial t} + \frac{\partial}{\partial x}(n_c v_c) = 0 \tag{1}$$

$$\frac{\partial v_c}{\partial t} + v_c.\frac{\partial v_c}{\partial x} = \alpha\frac{\partial \psi}{\partial x} - \frac{\alpha}{\theta}\frac{1}{n_c}\frac{\partial n_c}{\partial x} \tag{2}$$

$$\frac{\partial n_b}{\partial t} + \frac{\partial}{\partial x}(n_b v_b) = 0 \tag{3}$$

$$\frac{\partial v_b}{\partial t} + v_b.\frac{\partial v_b}{\partial x} = \alpha\frac{\partial \psi}{\partial x} - \frac{\alpha}{\sigma}\frac{1}{n_b}\frac{\partial n_b}{\partial x} \tag{4}$$

$$\frac{(1+\alpha+\beta)}{\alpha}.n_h = e^{\psi} \tag{5}$$

$$\frac{\alpha}{(1+\alpha+\beta)}\frac{\partial^2\psi}{\partial x^2} = n_c + n_h + n_b - 1 \tag{6}$$

In the above set of Eqs. (1)–(6), $n_{c,h,b}$ are the cold, hot and beam electrons, $v_{c,b}$ are the velocities of cold and beam electrons and ψ is the potential. In the above equations, densities are normalized by unperturbed density n_{e0}, potential by $K_B T_h/e$, space coordinate by $\lambda_{Dh} = \left(\frac{\varepsilon_0 K_B T_h}{n_{h0} e^2}\right)^{1/2}$, velocity by electron acoustic speed $\left(v_{ea} = \left(\frac{n_{c0}}{n_{h0}}\right)^{1/2}\left(\frac{K_B T_h}{m_e}\right)^{1/2}\right)$, time by inverse of cold electron plasma frequency $\omega_{pe}^{-1} = \left(\frac{\varepsilon_0 m_e}{n_{c0} e^2}\right)^{1/2}$ and

$$\alpha = \frac{n_{h0}}{n_{c0}} \quad \beta = \frac{n_{b0}}{n_{c0}} \tag{7}$$

$$\theta = \frac{T_h}{T_c} \quad \sigma = \frac{T_h}{T_b} \tag{8}$$

In order to describe the evolution of finite amplitude electron acoustic waves, we use general method of reductive perturbation technique[18] and introduced the stretched coordinates as $\tau = \epsilon^{3/2} t$, $\xi = \epsilon^{1/2}(x - \lambda t)$, where ϵ is a small parameter measuring the weakness of nonlinearity and λ is wave speed normalized by electron acoustic speed. All dependent variables are expanded in the power series of 'ϵ' as

$$\left.\begin{aligned} n_c &= n_{c0} + \epsilon n_{c1} + \epsilon^2 n_{c2} + \cdots, \\ v_c &= \epsilon v_{c1} + \epsilon^2 v_{c2} + \cdots, \\ n_b &= n_{b0} + \epsilon n_{b1} + \epsilon^2 n_{b2} + \cdots, \\ v_b &= v_{b0} + \epsilon v_{b1} + \epsilon^2 v_{b2} + \cdots, \\ \psi &= \epsilon\psi_1 + \epsilon^2\psi_2 + \cdots \end{aligned}\right\} \tag{9}$$

Substituting the stretched coordinates and set of Eq. (9) into the basic set of Eqs. (1)–(6), we develop equations in numerous powers of ϵ. Equating the equations in lowest order of ϵ, we get $n_{c1} = a_1\psi_1$, $v_{c1} = a_2\psi_1$, $n_{b1} = a_3\psi_1$ and $v_{b1} = a_4\psi_1$, where

$$\left.\begin{aligned} a_1 &= \frac{-\alpha n_{c0}}{\left(\lambda^2 - \frac{\alpha}{\theta}n_{c0}^2\right)}, & a_2 &= \frac{-\alpha\lambda}{\left(\lambda^2 - \frac{\alpha}{\theta}n_{c0}^2\right)}, \\ a_3 &= \frac{-\alpha n_{b0}}{(\lambda - v_{b0})^2 - \frac{\alpha}{\sigma}n_{b0}^2}, & a_4 &= \frac{-\alpha(\lambda - v_{b0})}{(\lambda - v_{b0})^2 - \frac{\alpha}{\sigma}n_{b0}^2} \end{aligned}\right\} \tag{10}$$

To the next order in ϵ, we attain the following set of Eqs.

$$\frac{\partial n_{c1}}{\partial \tau} - \lambda\frac{\partial n_{c2}}{\partial \xi} + n_{c0}\frac{\partial v_{c2}}{\partial \xi} + \frac{\partial}{\partial \xi}n_{c1}v_{c1} = 0, \tag{11}$$

$$\frac{\partial v_{c1}}{\partial \tau} - \lambda\frac{\partial v_{c2}}{\partial \xi} + v_{c1}\frac{\partial v_{c1}}{\partial \xi} - \alpha\frac{\partial \psi_2}{\partial \xi} + \frac{\alpha}{\theta}n_{c0}\frac{\partial n_{c2}}{\partial \xi} - \frac{\alpha}{\theta}n_{c1}\frac{\partial n_{c1}}{\partial \xi} = 0, \tag{12}$$

$$\frac{\partial n_{b1}}{\partial \tau} - (\lambda - v_{b0})\frac{\partial n_{b2}}{\partial \xi} + n_{b0}\frac{\partial v_{b2}}{\partial \xi} + \frac{\partial}{\partial \xi}n_{b1}v_{b1} = 0, \tag{13}$$

$$\frac{\partial v_{b1}}{\partial \tau} - (\lambda - v_{b0})\frac{\partial v_{b2}}{\partial \xi} + v_{b1}\frac{\partial v_{b1}}{\partial \xi} - \alpha\frac{\partial \psi_2}{\partial \xi} + \frac{\alpha}{\sigma}n_{b0}\frac{\partial n_{b2}}{\partial \xi} - \frac{\alpha}{\sigma}n_{b1}\frac{\partial n_{b1}}{\partial \xi} = 0. \tag{14}$$

$$\frac{\alpha}{1+\alpha+\beta}\frac{\partial^2\psi_1}{\partial \xi^2} = n_{c2} + n_{b2} + \frac{\alpha}{1+\alpha+\beta}\psi_2 + \frac{\alpha}{2(1+\alpha+\beta)}\psi_1^2 \tag{15}$$

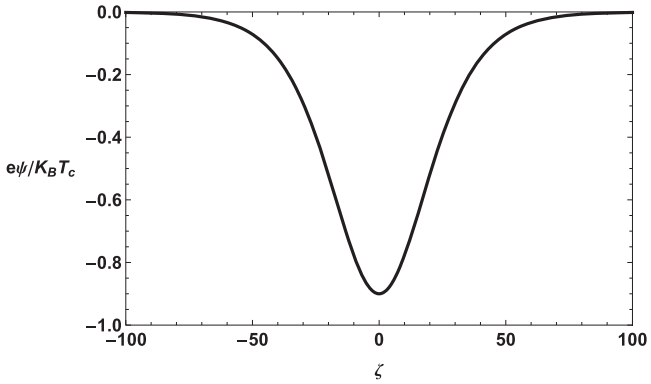

FIG. 1. Rarefactive electron acoustic solitary structure (EAS) studied by KdV equation when θ=100, σ=100, α=0.04, β=1, v_{b0}/V_{Tc}=5, and u=0.003.

Eliminating the second order potential quantities from the above set of Eqs. (11)–(15) by using first order quantities, we can obtain the KdV-equation in the first order perturbed potential as:

$$\frac{\partial \psi_1}{\partial \tau} + A\frac{\partial \psi_1^2}{\partial \xi} + B\frac{\partial^3 \psi_1}{\partial \xi^3} = 0, \tag{16}$$

where $A = b_2/b_1$ and $B = b_3/b_1$. The value of b_1, b_2 and b_3 are given bellow

$$b_1 = \left[\frac{a_3}{(\lambda - v_{b0})}\left(1 - \frac{n_{b0}}{\sigma}a_3\right) - \frac{a_3 a_4}{\alpha} + \frac{a_1}{\lambda}\left(1 - \frac{n_{c0}}{\theta}a_1\right) - \frac{a_1 a_2}{\alpha}\right], \tag{17}$$

$$b_2 = \left[\frac{a_3 a_4}{(\lambda - v_{b0})}\left(1 - \frac{n_{b0}}{\sigma}a_3\right) - \frac{a_3 a_4^2}{2\alpha} + \frac{a_3^3}{2\sigma} + \frac{a_1 a_2}{\lambda}\left(1 - \frac{n_{c0}}{\theta}a_1\right) + \frac{a_1^3}{2\theta} - \frac{a_1 a_2^2}{2\alpha} + \frac{\alpha}{2(1+\alpha+\beta)}\right], \tag{18}$$

and

$$b_3 = -\frac{\alpha}{(1+\alpha+\beta)}, \tag{19}$$

The solution of KdV Eq. (16) is

$$\psi = \frac{3u}{A}Sech^2\left[\frac{\xi}{\Delta}\right] \tag{20}$$

Here u is the velocity of the nonlinear structure and $\Delta = (4B/u)^{1/2}$ is the width of the solitary structure. We have solved Eq. (20) numerically and obtained rarefactive solitary structure of electron acoustic waves as shown in Fig. 1.

III. SIMULATION SETUP AND RESULTS

One dimensional electrostatic PIC **simulations** are carried out, which allows spatial variations along the x-axis[20] and neglected the ambient magnetic field. Initially the electrons are loaded into the grids assuming they follow Maxwellian velocity distribution function. We have **set** the periodic boundary condition. **In simulations, the unperturbed densities of hot (n_{h0}), cold (n_{c0}) and beam (n_{b0}) electrons are normalized by total unperturbed electron density n_{e0}[= n_{h0} + n_{c0} + n_{b0}], velocities by electron thermal velocity V_{Tc}, space coordinate by Debye length λ_{Dc}[= $(\varepsilon_0 T_C K_B/e^2 n_{c0})^{1/2}$] and time by $\omega_{pe}^{-1}\left[= \left(\varepsilon_0 m_e/e^2 n_{e0}\right)^{1/2}\right]$, respectively**. The electric field (E_x) and potential (ψ) are normalized by $\omega_{pe}V_{Tc}m_e/e$ and $K_B T_c/\varepsilon_0 e$ respectively. The time step is taken as 0.02 ω_{pe}^{-1} and the total number of particles utilized are 13,107,200 where the number of cells N_x =1024 with the grid spacing size λ_{Dc}. The parameters used in this model are given in Table I and Run 1 is taken as a reference case.

TABLE I. Simulation parameters for Run 1-3.

Run	θ	σ	α	β	v_{b0}/V_{Tc}
1	100	100	0.04	1	20
2	100	100	0.04	1	18
3	100	100	0.04	1	5

Figure 2 depicts the plot of electric field energy ($\varepsilon_p = E^2\varepsilon_0/2k_B T_c n_0$) on a log scale against normalized time ($\omega_{pe}t$) for Run 1. **Initially, the electric field energy** is linearly increased and at $\omega_{pe}t$ ~ 84.12 its value reaches to 0.0414. From $\omega_{pe}t$ ~ 84.12 to $\omega_{pe}t$ ~ 1275, the electric field energy decreases. However, a slight increase in energy is also observed after 1350. From Fig. 2 we can note that the electric field energy first shows linear increase up to $\omega_{pe}t$ ~ 84.12 and then nonlinear behavior for $\omega_{pe}t$ > 84.12. In Fig. 3(a)–3(d) electric field (E_x) and electrostatic potential (ψ) at $\omega_{pe}t$ = 50 and $\omega_{pe}t$ = 1400 for Run 1 are shown. Figure 3(a) and 3(b) describe the profile of the electric field and electrostatic potential at $\omega_{pe}t$ = 50 respectively. During this time, the oscillatory structure of the electric field is observed and similar behavior is seen in the electrostatic potential. This stage corresponds to the linear regime of the wave shown in Fig. 1. Figure 3(c) shows the four spikes of the bipolar electric field structures at $\omega_{pe}t$ = 1400. These bipolar structures are the electrostatic solitary (ES) structures which exactly coincides with the earlier results generated by fluid simulation[10] and observation results studied by many authors.[3,21–23] The profile of electrostatic potential at $\omega_{pe}t$ = 1400 corresponding to Fig. 3(c)

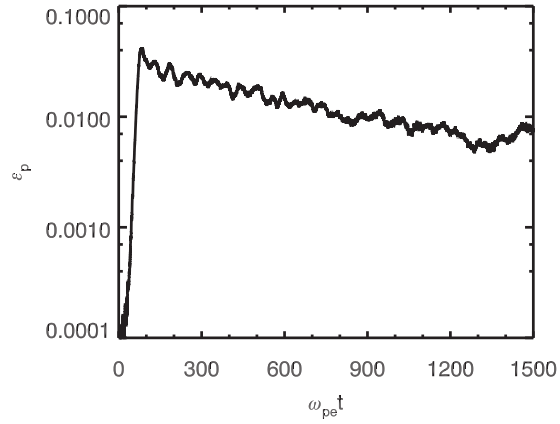

FIG. 2. Normalized electric (E_x) field energy ($\varepsilon_p = E^2\varepsilon_0/2k_B T_c n_0$) in log scale versus time evolution ($\omega_{pe}t$) for Run 1.

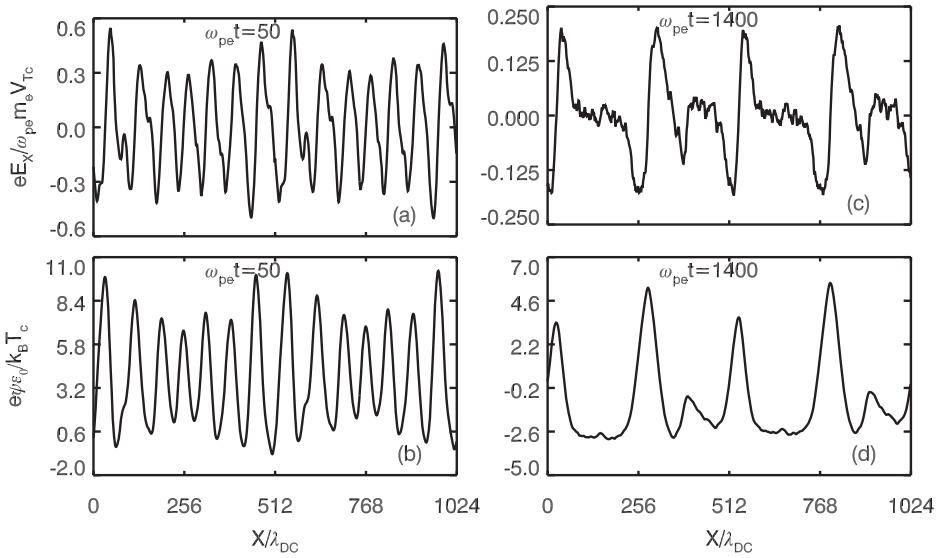

FIG. 3. Evolution of electric field (E_x) and electrostatic potential (ψ) (a and b) at $\omega_{pe}t$ = 50 and (c and d) at $\omega_{pe}t$ = 1400 for Run 1.

is shown in Fig. 3(d) which shows compressive solitary structures (divergent electric field configuration). Such compressive solitary structures have recently been reported in a theoretical study by Shah et al.[18] The formation of four positive peaks of electrostatic potential (Fig. 3(d)) exactly correspond to the four spikes of electric field plot (Fig. 3(c)). From Figs. 3(c) and 3(d) we can notice that these ES structures seem to be more self-consistent.

In order to understand the effects of cold electrons on the propagation of EA waves, we have plotted Fig. 4 which displays the phase-space portrait at different normalized times $\omega_{pe}t$ (=50 and 1400) using the plasma parameters of Run 1 shown in Table I. Initially the cold electrons follow the Maxwellian velocity distribution. For finite times, the wave-particle interaction leads to nonlinear structures. The wave then attain its saturation level at normalized time 1400 and consequently, maximum cold electrons in phase space finally give rise to thermalization or electron heating. Figure 5(a) and (b) displays the electric field (E_x) and electrostatic potential (ψ), respectively for Run 2. In the Run 2, we change the beam electron drift speed v_{b0} = 18 V_{tc} while other parameters used here are the same as in Run 1. It is also observed that for small reduction in the value of v_{b0} as compare to Run 1, the number of bipolar structures

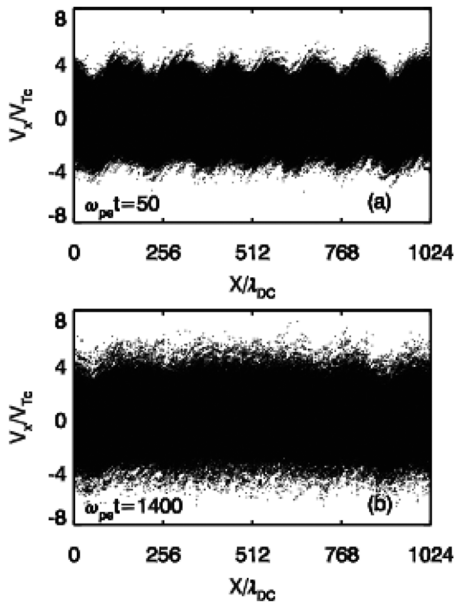

FIG. 4. The phase-space (x,v_x) plots for the cold electrons at $\omega_{pe}t$=50 and 1400 for Run 2.

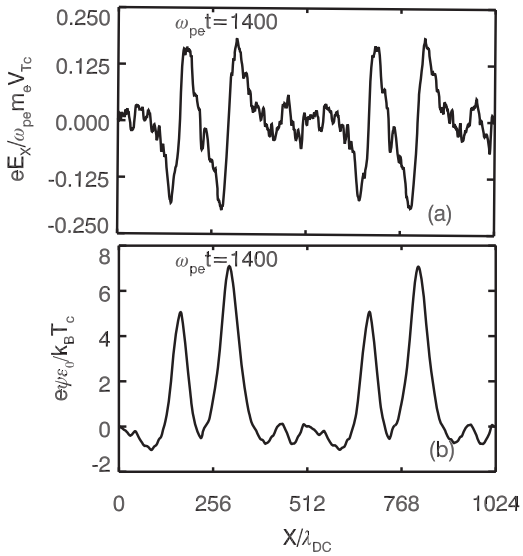

FIG. 5. Evolution of (a) electric field (E_x) and (b) electrostatic potential (ψ) at $\omega_{pe}t$ = 1400 Run 2.

and their amplitude remains the same but now they move in pairs instead of separately. In Fig. 5(b), the corresponding electrostatic potential is shown.

It has been studied by many authors[18,19] that the polarity of the solitary structures can be reversed, depending on the drift velocity of electron beam. The same can be confirmed from Fig. 6 where by further decreasing the drift velocity of electron beam v_{b0} = 5 for Run 3 the polarity of the structures are reversed. Figures 6(a) and 6(b) represent the electric field E_x and electrostatic potential ψ at $\omega_{pe}t$ = 1400. It is found that for a small value of electron beam velocity, the ES structures can also be generated and propagate in positive x-direction. It can be seen from Fig. 6(b) that unlike Fig. 3(d) and Fig. 5(b), the rarefactive solitary structures are formed (convergent electric field configuration). The blue arrow in the Figure 6 indicates rarefactive solitary structures. We believe that these structures are formed due to the contribution of EA waves, which agrees with the rarefactive (negative electrostatic potential) solitary solution of the KdV equation (see Fig. 1).

The nonlinear behavior of EA waves studied by KdV equation illustrates that EA waves evolve into EAS structure when its amplitude is large. The formation of electron-acoustic solitary structures is due to the steepening behavior of quasi-monochromatic EA waves. This kind of steepening already exist in sound waves[24] magnetosonic[25] and ion-acoustic waves.[26] At $\omega_{pe}t$ = 1410 the profiles of E_x and ψ show the same behavior as shown in Figs. 6(c) and (d), respectively.

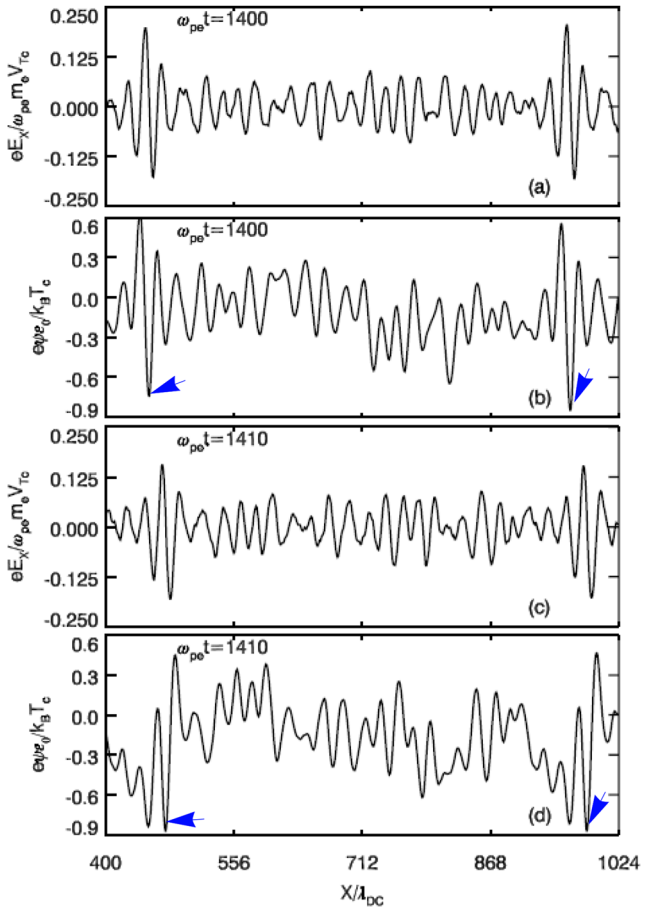

FIG. 6. Evolution of electric field (E_x) and electrostatic potential (ψ) (a and b) at $\omega_{pe}t$ = 1400 and (c and d) at $\omega_{pe}t$ = 1410 for Run 3.

IV. SUMMARY AND CONCLUSION

In this paper, we have presented the mechanism for the formation of compressive and rarefactive electrostatic solitary structures with 1D PIC simulations in an unmagnetized plasma, **consisting of immobile ions and** three Maxwellian electron populations, the cold, hot and beam electrons. We also derived the KdV equation for electron acoustic waves in an unmagnetized three component plasma in similar plasma conditions and obtained rarefactive solitary (negative electrostatic potential) structures. Simulations results showed that the electric potential of the ES waves is more positive than negative and shows a compressive solitary structures (divergent electric field configuration) for large value of electron beam velocity. For the first time, we found that for small value of beam velocity, rarefactive ES structures (convergent electric field configuration) are formed which agree with negative potential solitary structures obtained theoretically. We concluded that the rarefactive solitary structures are formed due to the steepening of EA waves. The steepening of EA waves is similar to steepening in sound waves[24] magnetosonic,[25] ion acoustic[26] and dust acoustic[27] waves in plasmas. We also found that the change in the polarity of solitary structures depends on the drift velocity of electron beam as observed earlier. The steepening of EA waves and formation of electric field spikes are **consistent** with the ES waves observation from Earth's magnetosphere.[23,28] In this study, we have performed kinetic simulations that agrees with the theoretical results in particular and from space observations in general.

ACKNOWLEDGMENTS

A. A. Abid acknowledges the Chinese Academy of Science (CAS) and TWAS for supporting him for a Ph.D. degree from University of Science and Technology of China in the category of 2016 CAS-TWAS President's Fellowship Awardee (Series No. 2016-172). This work is also supported by the NSFC grant 41331067, 41774169, 41527804, nd Key Research Program of Frontier Sciences, CAS (QYZDJ-SSW-DQC010).

REFERENCES

[1] J. Pickett, J. Menietti, D. Gurnett, B. Tsurutani, P. Kintner, E. Klatt, and A. Balogh, Nonlinear Processes in Geophysics **10**(1-2), 3–11 (2003).
[2] J. R. Franz, P. M. Kintner, and J. S. Pickett, Geophysical Research Letters **25**(8), 1277–1280, https://doi.org/10.1029/98gl50870 (1998).
[3] H. Matsumoto, Geophys. Res. Lett. **21**, 2915, https://doi.org/10.1029/94GL01284 (1994).
[4] S. Bale, P. Kellogg, D. Larsen, R. Lin, K. Goetz, and R. Lepping, Geophysical Research Letters **25**(15), 2929–2932, https://doi.org/10.1029/98gl02111 (1998).
[5] S. R. Bounds, R. F. Pfaff, S. F. Knowlton, F. S. Mozer, M. A. Temerin, and C. A. Kletzing, Journal of Geophysical Research: Space Physics **104**(A12), 28709–28717, https://doi.org/10.1029/1999ja900284 (1999).

[6]Q. Lu, D. Wang, and S. Wang, Journal of Geophysical Research: Space Physics **110**, A03223 (2005).
[7]A. Mangeney, C. Salem, C. Lacombe, J.-L. Bougeret, C. Perche, R. Manning, P. Kellogg, K. Goetz, S. Monson, and J.-M. Bosqued, Annales Geophysicae **17**, 307 (1999).
[8]F. Verheest, T. Cattaert, and M. A. Hellberg, Space Science Reviews **121**(1-4), 299–311 (2005).
[9]A. Kakad, S. Singh, R. Reddy, G. Lakhina, S. Tagare, and F. Verheest, Physics of Plasmas **14**(5), 052305 (2007).
[10]C. Dillard, I. Vasko, F. Mozer, O. Agapitov, and J. Bonnell, Physics of Plasmas **25**(2), 022905 (2018).
[11]Q. Lu, B. Lembège, J. Tao, and S. Wang, Journal of Geophysical Research: Space Physics **113**, A11219, https://doi.org/10.1029/2008ja013693 (2008).
[12]Q. Lu, S. Wang, and X. Dou, Physics of Plasmas **12**(7), 072903 (2005).
[13]S. P. Gary and R. L. Tokar, The Physics of Fluids **28**(8), 2439–2441 (1985).
[14]R. Mace and M. Hellberg, Journal of Plasma Physics **43**(2), 239–255 (1990).
[15]R. L. Tokar and S. P. Gary, Geophysical Research Letters **11**(12), 1180–1183, https://doi.org/10.1029/gl011i012p01180 (1984).
[16]M. Berthomier, R. Pottelette, M. Malingre, and Y. Khotyaintsev, Physics of Plasmas **7**(7), 2987–2994 (2000).
[17]I. Naeem, S. Ali, P. Sakanaka, and A. M. Mirza, Physics of Plasmas **24**(4), 042109 (2017).
[18]K. Shah, M. Qureshi, W. Masood, and H. Shah, Physics of Plasmas **25**(4), 042303 (2018).
[19]S. El-Labany, W. El-Taibany, and O. El-Abbasy, Physics of Plasmas **12**(9), 092304 (2005).
[20]Q. M. Lu and D. S. Cai, Computer Physics Communications **135**(1), 93–104 (2001).
[21]R. Ergun, C. Carlson, L. Muschietti, I. Roth, and J. McFadden, Nonlinear Processes in Geophysics **6**(3-4), 187–194 (1999).
[22]R. Ergun, C. Carlson, J. McFadden, F. Mozer, G. Delory, W. Peria, C. Chaston, M. Temerin, I. Roth, and L. Muschietti, Geophysical Research Letters **25**(12), 2041–2044, https://doi.org/10.1029/98gl00636 (1998).
[23]I. Vasko, O. Agapitov, F. Mozer, J. Bonnell, A. Artemyev, V. Krasnoselskikh, G. Reeves, and G. Hospodarsky, Geophysical Research Letters **44**(10), 4575, https://doi.org/10.1002/2017gl074026 (2017).
[24]L. Landau and E. Lifshitz, *F. Mechanics*, P. Press, Massachusetts (1959).
[25]R. Sagdeev, Rev Plasma Phys **4**, 23 (1966).
[26]D. Montgomery, Physical Review Letters **19**(26), 1465 (1967).
[27]J. Heinrich, S.-H. Kim, and R. Merlino, Physical Review Letters **103**(11), 115002 (2009).
[28]O. Agapitov, V. Krasnoselskikh, F. Mozer, A. Artemyev, and A. Volokitin, Geophysical Research Letters **42**(10), 3715–3722, https://doi.org/10.1002/2015gl064145 (2015).